

Binding energies of excitons in polar quantum well heterostructures

R. T. Senger* and K. K. Bajaj

Department of Physics, Emory University, Atlanta, Georgia 30322, USA

(Received 18 June 2003; published 20 November 2003)

We present a calculation of the variation of the binding energy of a heavy-hole exciton in a highly ionic quantum well structure, as a function of well width using a variational approach. We include the effects of exciton-phonon interaction and of mismatches between the particle masses and the dielectric constants of the well and barrier layers. The effect of exciton-phonon interaction is described in terms of an effective potential between the electron and the hole, derived by Pollmann and Büttner [J. Pollmann and H. Büttner, *Phys. Rev. B* **16**, 4480 (1977)] using an exciton–bulk optical-phonon Hamiltonian. We find that the values of the exciton binding energies we calculate agree very well with those obtained using a more rigorous but a complicated approach due to Zheng and Matsuura [R. Zheng and M. Matsuura, *Phys. Rev. B* **58**, 10 769 (1998)] in which they consider an exciton interacting with the confined-longitudinal optical phonons, interface phonons, and half-space phonons. Our method has the advantage of being considerably simpler, more efficient to use and is much easier to generalize to include the effects of external perturbations such as electric and magnetic fields. We compare the results of our calculations with the available experimental data in a few ionic quantum well structures and find a very good agreement. We show that for an appropriate understanding of the experimental data in ionic quantum well structures one must properly account for the exciton-phonon interaction.

DOI: 10.1103/PhysRevB.68.205314

PACS number(s): 78.66.Hf, 71.35.Cc, 63.20.Ls, 78.67.De

I. INTRODUCTION

Quantum well heterostructures based on wide band-gap materials, such as (Cd,Zn)O/(Mg,Zn)O, Zn(Cd,Se)/Zn(S,Se), and (In,Ga)N/(Al,Ga)N, are important for their potential applications in the fabrication of optical and electro-optical devices operating in the green-ultraviolet region of the electromagnetic spectrum. Besides, in (Cd,Zn)O/(Mg,Zn)O and Zn(Cd,Se)/Zn(S,Se) based quantum well (QW) heterostructures the radiative recombination of excitons can play an important role in lasing-emission processes.^{1,2} Exciton transitions have higher oscillator strengths and more peaked density of states than those corresponding to free carriers. In addition, the energy distribution of optical gain is much larger than that for the free-carrier recombination. Thus a lasing process based on excitonic recombination is expected to have a higher gain and a lower threshold. In particular, in ZnO based heterostructures, excitons can be responsible for optical processes at temperatures significantly higher than the room temperature (RT), since the exciton binding energy in bulk ZnO is 59 meV.³ These strongly polar heterostructures have recently attracted a great deal of interest,^{4–16} since they could be a valid alternative to (In,Ga)N/(Al,Ga)N QW heterostructures where excitons do not play an important role due to smaller values of the exciton binding energies and the presence of strong built-in electric fields throughout the structure.^{17,18} In fact, the improved quality of epitaxial growth techniques for ZnO based semiconductor alloys have recently led to the fabrication of high quality multiple quantum well (MQW) heterostructures with very good (in-plane) lattice match.^{6–16} The use of ScAlMgO₄ (SCAM) as a substrate, rather than sapphire, has greatly improved the properties of epitaxial ZnO and Mg_xZn_{1-x}O films in terms of surface flatness, crystal quality, electron mobility, and optical spectra, due to excellent lattice matching.⁶ Measurements of photoluminescence (PL) and absorption spectra in

ZnO/Mg_xZn_{1-x}O MQW's have clearly shown the quantum confinement effect and excitonic transitions up to RT (Ref. 6) and, recently, Makino and co-workers⁸ have reported RT excitonic stimulated emission in ZnO/Mg_{0.12}Zn_{0.88}O MQW heterostructures and measured thresholds below 22 kW/cm² for well widths in the range 7–47 Å, with a minimum of 11 kW/cm² for the 47 Å thick QW.

Therefore a proper understanding of the effective electron-hole interaction in these heterostructures is very important since it is necessary for the correct interpretation of the optical data as well as for improving the tailoring of the material properties, in view of their many device applications. In fact, due to the strongly polar nature of these systems, some effects usually neglected in III-V semiconductor heterostructures, such as exciton-phonon interaction, become important and not accounting for these effects properly can lead to a lack of accuracy in the interpretation of experimental data.

Various calculations of the exciton binding energies have been presented to interpret experimental data obtained in ZnCdSe/ZnSe QW heterostructures,^{19,20} leading to different levels of agreement according to the choices of physical parameters and the completeness of the models used for the calculations. We will show that accounting for the exciton-phonon interaction improves this agreement and reduces uncertainty in the values of physical parameters.

In this paper we present a calculation of the binding energy of a heavy-hole exciton as a function of well width in a highly ionic quantum well structure. We follow a variational approach and include the effects of the exciton-phonon interaction and of the mismatches between the particle masses and the dielectric constants between the well and the barrier layers. The effect of the exciton–longitudinal optical (LO) phonon interaction is described by means of an effective potential between an electron and a hole as derived by Pollmann and Büttner^{21,22} using the exciton–bulk-longitudinal

optical-phonon Hamiltonian. The effect of the dielectric mismatch on the binding energy of the exciton is calculated following the approach used by Kumagai and Takagahara.²³ We show that the values of the exciton binding energies we calculate agree very well with those obtained by considering an exciton interacting with confined-LO phonons, interface phonons, and half-space phonons.²⁴ Our method has the great advantage of being considerably simpler than the more rigorous but complicated approach of Zheng and Matsuura²⁴ and is much easier to generalize to include the effects of external perturbations such as electric and magnetic fields. We compare the results of our calculations with the available experimental data in several ionic quantum well structures and find a very good agreement. And finally we comment briefly on the validity of the approximations made in our calculations.

II. THEORY

The Hamiltonian of an electron-hole pair created in a quantum well, describing the excitonic state in interaction with the phonon modes of the polar medium, within the framework of effective-mass and decoupled valance-band approximations, can be expressed as composed of three parts; the exciton part containing kinetic energy, Coulomb interaction, and quantum well confinement potentials of the electron and the hole, phonon part describing the Hamiltonian of phonon field with components of confined, half-space, and interface modes, and finally the part corresponding to the interaction of the exciton with those phonon modes expressed in the form of well-known Fröhlich interaction Hamiltonian,

$$H = H_{\text{ex}} + H_{\text{ph}} + H_{\text{ex-ph}}. \quad (1)$$

Detailed explicit form of the above Hamiltonian is given in several works such as the one by Zheng and Matsuura.²⁴ The Hamiltonian that will be used in our calculations, however, is a formally simpler one which describes the effects of exciton-phonon coupling through an effective interaction potential between the electron and the hole, and polaronic self-energy contributions. Such an effective Hamiltonian which describes the excitons in bulk ionic media and successfully explains the measured values of the exciton binding energies in polar materials is derived by Pollmann and Büttner.^{21,22} Investigating the quantitative agreement between the results of original Hamiltonian (1) and of Pollmann-Büttner (PB) Hamiltonian based on bulk-phonon approximation is among the motivations of the present study. To account for the quantum well confinement potential we will employ an appropriately modified form of the PB effective Hamiltonian.

The heterostructure is made up of two different polar semiconductors having distinctive material parameters and band-gap energies. Assuming a type-I band alignment, the electron and the hole in the quantum well experience finite-barrier confinement potentials of the form

$$V_i^{\text{conf}}(z_i) = \begin{cases} 0, & |z_i| \leq L/2 \\ v_i, & |z_i| > L/2 \end{cases} \quad (i = e, h), \quad (2)$$

where ($i = e, h$) denote the electron and the hole, v_e and v_h are the conduction- and valence-band offsets, respectively. With the origin taken at the center of the quantum well of thickness L and positioning the well in the $x-y$ plane, the position coordinates of the particles are given by the vectors $\vec{r}_i = (\vec{\rho}_i, z_i)$. The total effective Hamiltonian of the system, taking into account the mass-mismatch and dielectric-mismatch effects, can be expressed in terms of the relative position vector $\vec{r} = \vec{r}_e - \vec{r}_h = (\vec{\rho}, z)$ and the particle coordinates as

$$H_{\text{eff}} = \sum_{i=e,h} \left[-\frac{\hbar^2}{2} \frac{\partial}{\partial z_i} \frac{1}{m_i(z_i)} \frac{\partial}{\partial z_i} + V_i^{\text{conf}}(z_i) \right] - \frac{\hbar^2}{2\mu} \frac{1}{\rho} \frac{\partial}{\partial \rho} \rho \frac{\partial}{\partial \rho} + V_{\text{KT}}(\rho, z_e, z_h; \xi) + V_{\text{PB}}(r; a_{\text{ex}}) + E_{\text{self}}(\alpha_e, \alpha_h; a_{\text{ex}}). \quad (3)$$

The position dependences of the electron mass and the hole mass along the z direction are defined through their corresponding values in the well (w) and the barrier (b) regions,

$$m_i(z_i) = \begin{cases} m_i^w, & |z_i| \leq L/2 \\ m_i^b, & |z_i| > L/2 \end{cases} \quad (i = e, h). \quad (4)$$

μ is the reduced mass corresponding to heavy-hole bands in the plane perpendicular to the z axis. Both μ and m_h^j ($j = w, b$) can be expressed in terms of the well-known Luttinger band parameters^{25,26} of the well and barrier materials,

$$\frac{1}{\mu} = \frac{1}{m_e^w} + \frac{1}{m_0} (\gamma_1^w + \gamma_2^w), \quad (5)$$

$$\frac{1}{m_h^j} = \frac{1}{m_0} (\gamma_1^j - 2\gamma_2^j) \quad (j = w, b), \quad (6)$$

where m_0 is the free-electron mass.

The Coulomb interaction between the electron and the hole is modified in a quantum well due to penetration of their electric fields through a dielectric discontinuity. In the presence of two media with different dielectric constants each charge induces a different polarization, which leads to a charge distribution at the interface. When a layer is sandwiched by a material with a smaller dielectric constant, the fields produced by the charge distributions at the interfaces force the electron and the hole into the middle of the central layer, modify their Coulomb field and enhance their interaction. To describe this effect we adopt the approach presented by Kumagai and Takagahara (KT),²³ who studied in detail the effects of the dielectric confinement on the electron-hole Coulomb interaction, treating the dielectric mismatch by means of the image charge method. Using this technique they calculated the effective Coulomb potential throughout the quantum well heterostructure, describing the actual field by introducing a number of virtual charges whose positions and charge values satisfy the continuity of the macroscopic electric field across the boundaries. In the case of a quantum

well, due to the presence of two interfaces the resulting potential consists of a series of infinite terms, whose complete expressions are given in Ref. 23 and represented in Hamiltonian (3) by the term $V_{\text{KT}}(\rho, z_e, z_h; \xi)$. It should be noted that in Eq. (3) the direct Coulomb interaction term is already contained in the PB potential, and hence is excluded from V_{KT} . The relative importance of the effect of the dielectric mismatch depends on the argument $\xi = (\epsilon_0^w - \epsilon_0^b) / (\epsilon_0^w + \epsilon_0^b)$ of V_{KT} , which vanishes if the static dielectric constants of the well and barrier materials, ϵ_0^j ($j = w, b$), are assumed to be equal.

As mentioned above the PB effective potential $V_{\text{PB}}(r; a_{\text{ex}})$ together with the self-energy term describes the polaronic effects on the exciton ground state. The expression of the potential was originally derived for bulk media assuming an isotropic hole mass, and has a spherically symmetric form as a function of the relative distance between the electron and the hole. The other argument a_{ex} is called the exciton size, and its value depends on the particular form of the exciton wave function. In principle, the effective Hamiltonian of polaronic exciton can be rederived with the relevant wave function and the appropriate symmetry of the quantum well system. However, such a calculation turns out to be more tedious and complicated than dealing with the original Hamiltonian of the problem. Therefore we choose to keep the form of the potential as derived for bulk, but let the quantum well confinement to act through the parameter a_{ex} by its generalized redefinition. The material parameters appearing in the PB potential are taken as those of the well material, such as the electron mass $m_e^* = m_e^w$, and the value of the hole mass is taken as the weighted average of its values along the z and transverse directions, which can be expressed simply in terms of the Luttinger parameter as $m_h^* = m_0 / \gamma_1^w$.²⁶ With these approximations the PB potential and the self-energy terms are expressed as

$$V_{\text{PB}}(r; a_{\text{ex}}) = -\frac{e^2}{\epsilon_0^w r} - \frac{e^2}{\epsilon^* r} \left[\frac{C^4}{B^4} - \frac{m_e^* h_e}{\Delta m} e^{-rA_e/R_e} + \frac{m_h^* h_h}{\Delta m} e^{-rA_h/R_h} - \left(h_\mu + \frac{C^3 r}{2B^3 a_{\text{ex}}} \right) e^{-rB/R_\mu} \right], \quad (7)$$

$$E_{\text{self}}(\alpha_e, \alpha_h; a_{\text{ex}}) = -(\alpha_e g_e + \alpha_h g_h - \alpha_\mu g_\mu) \hbar \omega_{\text{LO}}, \quad (8)$$

where $\epsilon^* = (1/\epsilon_\infty^w - 1/\epsilon_0^w)^{-1}$, ϵ_0^w and ϵ_∞^w respectively, being the static and optical dielectric constants in the well and $\Delta m = m_h^* - m_e^*$ is the mass difference. Defining $M = m_e^* + m_h^*$ as the total mass, and $m_\mu^* = m_e^* m_h^* / M$ as the reduced mass, dimensionless charge-phonon coupling constants, and the characteristic polaron radii for the electron, the hole, and the reduced mass are given by

$$\alpha_i = \frac{e^2}{2\epsilon^* R_i \hbar \omega_{\text{LO}}},$$

$$R_i = \sqrt{\frac{\hbar}{2m_i^* \omega_{\text{LO}}}} \quad (i = e, h, \mu), \quad (9)$$

where ω_{LO} is the frequency of the dispersionless longitudinal optical phonons. The remaining coefficients have the following explicit forms:²²

$$A_i^2 = 1 + R_i^2 / a_{\text{ex}}^2 \quad (i = e, h),$$

$$B^2 = 1 + C^2, \quad C^2 = R_\mu^2 / a_{\text{ex}}^2,$$

$$h_i = 1 + (m_j^* R_i / m_i^* a_{\text{ex}})^2 \quad (j \neq i = e, h),$$

$$h_\mu = -(m_e^* / m_h^* + m_h^* / m_e^*) C^2 + C^4 / B^4,$$

$$g_i = A_i (1 - \frac{1}{2} R_i^2 / a_{\text{ex}}^2) \quad (i = e, h),$$

$$g_\mu = C^2 (4 + \frac{1}{2} C^2 + C^2 / B^2 - 2A_e d_e - 2A_h d_h) / B,$$

$$d_i = (1 + A_i B \sqrt{m_j^* / M}) / (A_i + B \sqrt{m_j^* / M}) \quad (j \neq i = e, h). \quad (10)$$

The effective interaction Hamiltonian defined above has an explicit and crucial dependence on the quantity a_{ex} . It is a measure of the size of the exciton, and its value is determined variationally. The PB effective Hamiltonian was derived for a bulk semiconductor using a one parameter hydrogenic trial wave function, $\Psi_{\text{bulk}}(r) = N \exp(-r/\lambda)$, where λ is a variational parameter. Consequently, the value of the exciton radius used in the effective Hamiltonian has a bulk limit given by $a_{\text{ex}} = \langle \Psi_{\text{bulk}} | 1/r | \Psi_{\text{bulk}} \rangle^{-1} = \lambda$. In the present case, however, the variational trial wave function we use also contains one-particle electron and hole envelope functions, and an extra variational parameter σ to account for the cylindrical symmetry of the quantum well geometry:

$$\Psi(r_e, r_h, r) = N \phi_e(z_e) \phi_h(z_h) \times \exp(-\sqrt{\rho^2 + \sigma^2(z_e - z_h)^2} / \lambda). \quad (11)$$

In the above, N is the normalization constant, $\phi_i(z_i)$ ($i = e, h$) are the one-particle ground-state solutions of the part of Hamiltonian (3) regarding the motion along the z direction. To account for the confinement effects we simply generalize the definition of the exciton size using the new wave function, $a_{\text{ex}}(\lambda, \sigma) = \langle \Psi | 1/r | \Psi \rangle^{-1}$. As expected, such a form will lead to the correct bulk limit for wide quantum wells for which $\phi_i(z_i)$ are almost constant, and the anisotropy parameter σ tends to one.

We should also note that in this treatment of the effective electron-hole interaction, the renormalization of the electron and hole masses to polaronic masses is not required as shown by Pollmann and Büttner in their work.²² The assumption that the above form of the effective potential which is derived for bulk is not significantly modified in the presence of an external confinement has been successfully used to describe the measured diamagnetic shifts in the case of a polaronic exciton in a magnetic field,²⁷ where the magnetic field provided the means of confinement in that case.

The ground-state energy of the system is obtained by minimizing the expectation value of the effective Hamiltonian, Eq. (3), with respect to the variational parameters,

$$E_0 = \min_{\lambda, \sigma} \langle \Psi | H_{\text{eff}}(\lambda, \sigma) | \Psi \rangle. \quad (12)$$

Since the phonon field and the coupling of the exciton to the phonons are included in the Hamiltonian, the variational ground-state energy E_0 is an upper bound to the energy of the polaronic exciton including the appropriate renormalization effects due to phonons.

Exciton binding energy is defined in reference to the energy of the state corresponding to uncorrelated electron and hole polarons in the quantum well,

$$E_B = E_e^{\text{sub}} + E_h^{\text{sub}} + E_e^{\text{pol}} + E_h^{\text{pol}} - E_0, \quad (13)$$

where E_i^{sub} ($i=e, h$) are the ground-state subband energies of the electron and the hole, calculated as the solutions of the Hamiltonian which is given as the first term of H_{eff} (3). For the polaron self-energies in a quantum well, as an approximation we use their corresponding bulk values, $E_i^{\text{pol}} = -\alpha_i \hbar \omega_{\text{LO}}$. It is well known²⁸ that the confined polarons in fact have somewhat lower self-energies, therefore the binding energies we calculate are expected to have slightly larger values for the intermediate values of the quantum well width.

The PB description of the exciton-phonon interaction in an ionic medium brings about significant improvements over some simplified approaches which describe the polaronic exciton as the interactions of two quasiparticles, an electron-polaron, and a hole-polaron, through a screened Coulomb potential. Appropriate particle mass values to be used in this model are the polaron masses given by

$$m_i^{\text{pol}} = m_i(1 + \alpha_i/6) \quad (i=e, h), \quad (14)$$

where coupling constants α_i are defined in Eq. (9), and the Coulomb interaction potential is taken as screened by the static dielectric constant, corresponding to the first term in V_{PB} , Eq. (7). Since the mutual interaction effects of the oppositely charged polarons are totally ignored, the corresponding polaronic self-energy of the exciton is assumed to be the sum of the self-energies of the individual polarons, $E_{\text{self}} = -(\alpha_e + \alpha_h) \hbar \omega_{\text{LO}}$. In the following, exciton binding energies as calculated using this ‘‘shallow exciton model’’ will also be presented for comparison purposes. Such simple models are in fact accurate enough for weakly polar materials like GaAs.

In more ionic materials, however, the Coulomb interaction between the electron and the hole as well as their polaronic self-energies become significantly modified, so that a more elaborated description such as that provided by PB effective Hamiltonian is required. Let us briefly review the details of how PB potential provides a successful description of exciton-phonon interaction, first in the bulk limit. The first term in the effective interaction potential (7) is in the form of static screening. As compared to the original form of Hamiltonian (1), the elimination of phonon coordinates to obtain an effective electron-hole interaction transforms the Cou-

lomb interaction from a dynamically screened to a statically screened one in the leading order.²² However the terms in V_{PB} as well as the self-energy expression, Eq. (8), are essential to describe the detailed and nontrivial interaction of the two charges with opposite polarization fields around them. The crucial parameter that determines the form of the effective interaction is the ratio of the effective exciton size a_{ex} to the polaron radii R_i . It is instructive to check the limiting cases of this ratio in an ionic material. In the limits of weak and strong binding it is easy to show that

$$\begin{aligned} \lim_{a_{\text{ex}}/R_i \rightarrow \infty} E_{\text{self}} &= -(\alpha_e + \alpha_h) \hbar \omega_{\text{LO}} \quad \text{and} \quad \lim_{a_{\text{ex}}/R_i \rightarrow 0} E_{\text{self}} \\ &= 0. \end{aligned} \quad (15)$$

For large exciton radii the total self-energy approaches the sum of the two individual self-energies of the free polarons. In the opposite limit for very small exciton radii the total self-energy of the exciton vanishes because the polarization clouds of the electron and the hole cancel each other. In general, and under the influence of the confinement potential, the partial cancellation of the polarization fields is well described by Eq. (8). Similarly, in these extreme limits the effective potential gets the following asymptotic forms:

$$\lim_{a_{\text{ex}}/R_i \rightarrow \infty} V_{\text{PB}}(r) = -\frac{e^2}{\epsilon_0^w r} - \frac{e^2}{\epsilon^* r} \frac{(m_h e^{-r/R_h} - m_e e^{-r/R_e})}{(m_h - m_e)}$$

and

$$\lim_{a_{\text{ex}}/R_i \rightarrow 0} V_{\text{PB}}(r) = -\frac{e^2}{\epsilon_\infty^w r}. \quad (16)$$

For extremely small sizes of the exciton, the effective Coulomb interaction becomes dynamically screened where the polaronic effects diminish entirely. With these reasonable limits, PB Hamiltonian gives a successful description of the polaronic excitons.²² In the present study the main effect of the confining potential is to modify the charge densities of both the electron and the hole, decreasing the relative distance between them; which in turn makes the effective electron-hole interaction potential to be less screened through the PB term.

III. RESULTS AND DISCUSSION

We have calculated the variation of the heavy-hole exciton binding energy E_B as a function of well width L in several ionic quantum well structures. The values of the various physical parameters used are given in Table I. In Fig. 1 we display the variation of the exciton binding energy as a function of well width in $\text{Zn}_{0.6}\text{Cd}_{0.4}\text{Se}/\text{ZnSe}$ quantum wells. The solid curve represents the results of our calculation including dielectric mismatch effect. We find, as expected, that the value of E_B increases as the well width is reduced, reaches a maximum and then drops rather sharply. This behavior of E_B with L was first observed and explained by Greene *et al.*²⁹ Open circles represent the results of Zheng and Matsuura²⁴

TABLE I. Values of the various physical parameters used in our calculation. All mass values are for corresponding band masses of the particles without polaronic corrections and are expressed in units of the free-electron mass. m_e^w and m_e^b are the isotropic conduction-band masses in the well and barrier regions, respectively. m_h^{\parallel} is the heavy-hole mass of the well material in the plane parallel to the quantum well, whereas the hole masses along the z direction in the well and barrier regions are denoted by m_h^w and m_h^b , respectively. The conduction- and valence-band offsets, v_e and v_h , and the LO-phonon energies of the well material are given in millielectron volt. All other symbols are defined in the text.

Well/Barrier	m_e^w	m_e^b	m_h^{\parallel}	m_h^w	m_h^b	ϵ_0^w	ϵ_{∞}^w	ϵ_0^b	v_e	v_h	$\hbar\omega_{\text{LO}}$
Zn _{0.6} Cd _{0.4} Se/ZnSe ^a	0.114	0.122	0.453	0.453	0.504	8.62	5.72	7.60	294	74	29.2
Zn _{0.69} Cd _{0.31} Se/ZnSe ^b	0.131	0.136	0.323	0.816	0.813	8.96	5.73	8.80	230	98	29.7
Zn _{0.77} Cd _{0.23} Se/ZnSe ^b	0.132	0.136	0.324	0.815	0.813	8.92	5.73	8.80	171	73	30.1
ZnO/Mg _{0.27} Zn _{0.73} O ^c	0.24	0.24	0.78	0.78	0.78	8.1	4.0	8.1	424	106	72.0
ZnO/Mg _{0.12} Zn _{0.88} O ^c	0.24	0.24	0.78	0.78	0.78	8.1	4.0	8.1	168	42	72.0
GaN/Al _{0.3} Ga _{0.7} N ^d	0.20	0.24	0.80	0.80	1.01	9.8	5.4	9.4	425	283	92.0

^aReference 24.

^bReferences 19, 20.

^cReference 11.

^dReference 41.

who consider the interaction of excitons with confined-LO phonons, interface phonons, and half-space phonons, and the effect of dielectric mismatch. We find an excellent agreement between our results obtained using PB potential and those calculated by Zheng and Matsuura. In Fig. 1 we have also plotted the variation of E_B with L as obtained using only PB potential (dot-dashed line), and static screened Coulomb potential with polaron mass (dashed line). First, we find that the values of E_B obtained using static screened Coulomb potential are considerably lower than those obtained by PB potential, thus emphasizing the importance of including the effect of exciton-phonon interaction in the calculation of the exciton binding energies. Second, we note that the effect of di-

electric mismatch on the values of E_B is quite significant in this quantum well structure.

In Fig. 2 we display the variation of the exciton binding energy as a function of well width in a Zn _{x} Cd _{$1-x$} Se/ZnSe quantum well structure using our full calculation (solid curves) and a static screened Coulomb potential (dashed curves) for Cd concentrations (x) of 31% and 23%. Our choice of the physical parameters are shown in Table I. In this case the Luttinger parameters of the well layer are calculated by linear interpolation between those for ZnSe ($\gamma_1 = 2.45, \gamma_2 = 0.61$) by Holscher *et al.*³⁰ and those for CdSe ($\gamma_1 = 2.52, \gamma_2 = 0.65$) by Fu *et al.*³¹ The use of these parameters leads to the hole masses which are almost identical in the well and barrier layers.

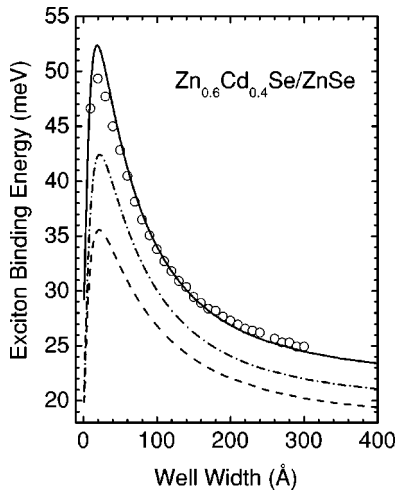


FIG. 1. Variation of exciton binding energy as a function of well width in a Zn_{0.6}Cd_{0.4}Se/ZnSe quantum well. The solid curve is obtained using PB potential and including dielectric mismatch effect. Open circles represent the results of an equivalent calculation by Zheng and Matsuura (Ref. 24). The dot-dashed and dashed curves are obtained using PB potential and static screened Coulomb potential, respectively, without the dielectric-mismatch effect.

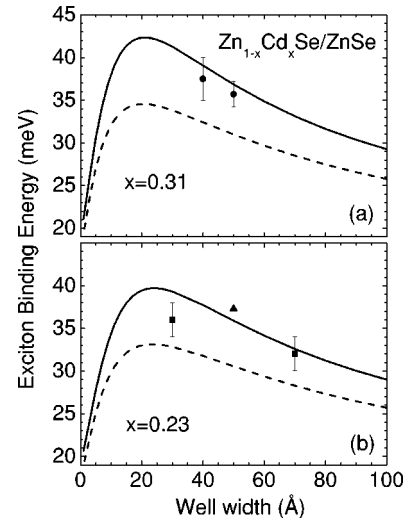


FIG. 2. Variation of exciton binding energy as a function of well width in Zn _{$1-x$} Cd _{x} Se/ZnSe quantum wells for $x = 0.31$ and $x = 0.23$. The solid curves represent our full calculations. The dashed curves are obtained using the shallow exciton model. The experimental data are represented by circles ($x = 0.31$, Ref. 19), squares ($x = 0.23$, Ref. 20), and a triangle ($x = 0.21$, Ref. 32).

In Fig. 2 symbols represent experimental data by De Nardis *et al.*¹⁹ ($x=31\%$, circles), Cingolani *et al.*²⁰ ($x=23\%$, squares), and Puls *et al.*³² ($x=21\%$, triangle). The results of our calculations for $x=21\%$ are not presented since the deviations from the results for $x=23\%$ are always less than 1 meV throughout the presented range of well widths. De Nardis *et al.*¹⁹ and Puls *et al.*³² determine the values of the exciton binding energies from the difference between the spectral positions of the $1s$ and $2s$ exciton states, since they studied the absorption as a function of magnetic field and were able to resolve the $2s$ state at high magnetic fields. Cingolani *et al.*,²⁰ on the other hand, determined the values of the exciton binding energies as the difference between the spectral position of the $1s$ state and the exciton continuum. It should be pointed out that the experimental determination of the electron and the hole masses actually refers to the polaron masses m_i^{pol} of the particles. Therefore we have calculated their band masses from the polaron masses reported in the literature using the relation given in Eq. (14), and derived the hole masses from Luttinger parameters. Values of the various physical parameters reported in literature for CdSe and ZnSe materials are strongly dependent on the experimental techniques used for their determination. This leads to rather large uncertainties, especially in the values of the masses and dielectric constants.^{19,20,30-34} A discussion of the Luttinger mass parameters of ZnSe as determined by different techniques can be found in Ref. 19.

It is clear from Fig. 2 that the experimental values of the exciton binding energies for 40 Å, 50 Å, and 70 Å well widths agree rather well with the results of calculations which include exciton-phonon interaction, whereas the exciton binding energies calculated assuming a static screened Coulomb interaction are too low. For a 30-Å well, however, the experimental value is somewhat lower than the calculated value. The absorption spectrum measured by Cingolani *et al.*²⁰ in this quantum well is rather broad. The strong overlap between the exciton resonance and the exciton continuum can lead to a considerable uncertainty in the determination of the exciton binding energy, which should be larger than the ± 2 meV reported in their work.

Some time ago Pelekanos *et al.*³⁴ studied the behavior of the $1s$ and the $2s$ states of an exciton in a 90 Å wide $\text{Zn}_{0.75}\text{Cd}_{0.25}\text{Se}/\text{ZnSe}$ quantum well structure as a function of the magnetic field, using absorption spectroscopy. They determine a value of 31 meV for the difference between these two transitions at zero magnetic field. By adding to this value the corresponding binding energy of the $2s$ state they obtain an exciton binding energy of 37 meV in this structure. This value is considerably larger than that calculated for a 90 Å wide well using any of the three sets of physical parameters mentioned above as well as its measured value in a 70 Å wide well.²⁰ The reason for this discrepancy is not clear though we suspect that the transition they identify as due to $2s$ state is probably incorrect. This is due to the fact that the diamagnetic shift they measure for this transition is too small for a $2s$ state.¹⁹ However, we find that the exciton binding energy calculated using the physical parameters proposed by Zheng and Matsuura²⁴ is close to the value determined from the data of Pelekanos *et al.*³⁴ It should be pointed out that

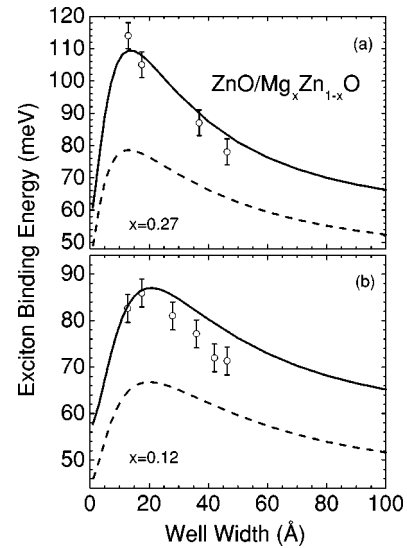


FIG. 3. Variation of exciton binding energy as a function of well width in $\text{ZnO}/\text{Mg}_x\text{Zn}_{1-x}\text{O}$ quantum wells for $x=0.27$ and $x=0.12$. The solid and dashed curves are obtained using PB and static screened Coulomb potentials, respectively. The symbols represent the experimental data by Sun *et al.* (Ref. 12).

values of the electron and hole masses used by Zheng and Matsuura are actually polaron masses and not the band masses as assumed by them. They also assume that the hole mass is isotropic. In addition, they use a value of ϵ_0 (7.6) that is considerably smaller than that used by many other groups. All these assumptions lead to considerably larger values of the exciton binding energies. It should be pointed out that in the calculations of the exciton binding energies displayed in Fig. 1 we have used the same values of the physical parameters as those used by Zheng and Matsuura as we are interested in comparing the results of our calculations with those of their calculations.

In Figs. 3(a) and 3(b) we display the variations of the binding energies of the heavy-hole excitons as a function of well width in two $\text{ZnO}/\text{Mg}_x\text{Zn}_{1-x}\text{O}$ quantum well heterostructures with $x=0.27$ and $x=0.12$, respectively. The choice of the various physical parameters used, as given in Table I, has been discussed in detail by Coli and Bajaj.¹¹ The conduction to valance-band offset ratio was used as an adjustable parameter as this value is not accurately known. A ratio of 80/20 is used in our calculations. The circles refer to the experimental data obtained by Sun *et al.*¹² using absorption measurements at 5 K. Their quantum well structures were grown by laser molecular beam epitaxy on SCAM substrates which have an excellent lattice matching with ZnO. The values of the well width ranged from 6.9 to 46.5 Å. The thickness of the barrier layers was kept at 50 Å in both sets of samples. Again the solid curves refer to the results of the calculation including exciton-phonon interaction using PB potential. The effects of the mismatches of the particle masses and the dielectric constants are not included as the values of these quantities are not known in MgZnO . The dashed curves refer to calculations where the electron-hole interaction is described by the static screened Coulomb potential and the polaron masses of the electrons and holes are

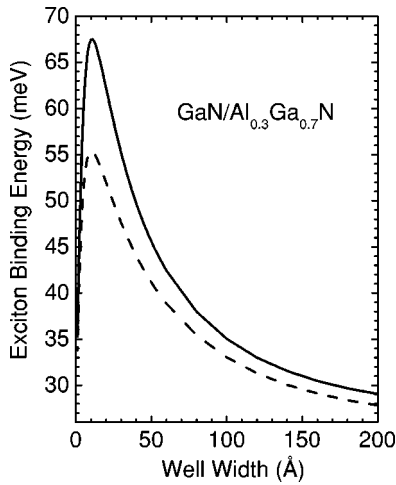


FIG. 4. Variation of exciton binding energy as a function of well width in a GaN/Al_{0.3}Ga_{0.7}N quantum well. The solid and dashed curves represent the results of PB and shallow exciton models, respectively, including the dielectric-mismatch effect.

used. As expected, the use of the screened Coulomb potential leads to a significant underestimation of the exciton binding energies as compared to those where the full electron-hole interaction is taken into account. It should be pointed out that Mg_xZn_{1-x}O alloy grows with wurtzite symmetry for values of $x \leq 0.5$.³⁵ The values of the physical parameters available in literature are for MgO which always grows with zincblende symmetry thus making it impossible to determine the physical parameters of the alloy system by interpolation. Finally we have assumed that there is no strain present in the well or in the barrier region as suggested in Ref. 5 and therefore no electric fields. However, recently Makino *et al.*¹⁴ have studied photoluminescence properties of a number of samples of ZnO/Mg_xZn_{1-x}O quantum well structures ($x = 0.12$ and 0.27) with various well widths of 7–46.5 Å. They find a significant presence of built-in electric fields due to piezoelectric and spontaneous polarization effects only in larger wells ($L > 42.3$ Å) and high Mg content ($x = 0.27$). As shown in Figs. 3(a) and 3(b) the values of the exciton binding energies measured by Sun *et al.*¹² agree very well with those calculated by us including the exciton-phonon interaction and are considerably larger than those obtained by using the static screened Coulomb potential.

In Fig. 4 we display the variations of the exciton binding energies as a function of well width in GaN/Al_{0.3}Ga_{0.7}N quantum well structures, using the physical parameters given in Table I and conduction to valance-band offset ratio of 60/40. Again the solid curve represents the results of the calculation which includes exciton-phonon interaction and the effects of mass and dielectric mismatches. Dashed curve represents the results obtained using static screened Coulomb potential. It is not possible for us to compare the results of our calculations with the experimental data as the measured values always include the effect of built-in electric fields due to piezoelectric and spontaneous polarizations. However, it is important to know the values of the exciton binding energies at zero field in order to determine their shifts for finite values of the electric field.

Finally, we would like to comment on the approximations we have made in our calculations. We have assumed parabolic conduction and valance bands and thus ignored the effects of nonparabolicity. Whenever known, we have used anisotropic values of the heavy-hole mass. We have not included the effects of the valance-band mixing in our calculations. These effects are known to enhance the values of the exciton binding energies depending on the valance-band structure.³⁶ We have used exciton–bulk-LO-phonon interaction as formulated by Pollmann and Büttner.²² In the expressions involving hole-LO-phonon interaction we have used average values of the anisotropic hole masses.

Some time ago Mori and Ando³⁷ investigated the behavior of electron-optical-phonon interaction in single and double heterostructures using a dielectric continuum model. One of the important results of their study is the sum rule of form factors which states that the sum of the contributions of all kinds of phonon modes is exactly equal to that of bulk modes if the coupling constants are assumed to be independent of the modes. Rucker *et al.*³⁸ using a fully microscopic model of a GaAs/Al_xGa_{1-x}As quantum well structure calculated numerical results which strongly supported the sum rule derived by Mori and Ando.³⁷ Register³⁹ studied the behavior of polar-optical-phonon scattering of carriers in heterostructures using a microscopic model and derived a sum rule analogous to that of Mori and Ando,³⁷ which is applicable to arbitrary heterostructure geometries and nonmetallic materials. It should be pointed out that in spite of the general validity of the above-mentioned sum rule, significant differences can occur between scattering rates (imaginary parts of the self-energies) calculated using models based on bulk phonons and those based on the phonon modes of the quantum well structures such as confined, interface, and half-space phonons because of the possible resonances between the sub-band energies and the phonon energies. However, the calculations of the real parts of the self-energies are inherently far less sensitive to such resonances. It is therefore not surprising that the values of the exciton binding energies we calculate using PB potential agree so well with those calculated by Zheng and Matsuura²⁴ using exciton interaction with confined-LO phonons, interface phonons, and half-space phonons. It is important to realize that our approach is easier to generalize to study the effects of applied external perturbations such as magnetic and electric fields on the properties of excitons in quantum well structures than that followed by Zheng and Matsuura.²⁴

We shall now briefly comment on the effect of high concentration of free carriers on the binding energy of excitons in quantum well laser structures based on highly ionic semiconductors. Under lasing conditions we have a highly complex many-body system with the simultaneous presence of excitons, free electrons, holes, and free optical phonons at finite temperatures. A proper calculation of the exciton binding energies as a function of carrier density in such a system is a formidable task. However, it is possible to make a few general qualitative observations. During the past 20 years a number of groups have investigated the behavior of this many-body system in the absence of optical phonons.⁴⁰ For instance, de-Leon and Laikhtman have calculated the varia-

tion of the exciton binding energy as function of free-carrier concentration at finite temperature in single quantum well structures. They consider three different screening models: (1) static screening without phase filling, (2) dynamic screening without phase filling factor, and finally (3) dynamic screening with phase filling factor. They find that the dynamic screening with phase filling is very effective in screening out the effective interaction between the electron and the hole. The exciton binding energy goes to zero at a critical value of the free-carrier concentration, which depends on the details of the quantum well structure and temperature. As they do not include the effects of exciton-phonon interaction and the presence of real phonons, it is not clear how the exciton binding energy will behave as a function of free-carrier concentration in such structures. The presence of free carriers also modifies the exciton-phonon interaction in highly ionic quantum well structures.

IV. CONCLUSIONS

We have calculated the variation of the binding energy of a heavy-hole exciton as a function of well width in quantum well structures composed of highly polar semiconductors. We follow a variational approach and include the effects of exciton–optical-phonon interaction and of the mismatches

between the particle masses and the dielectric constants between the well and the barrier layers. We describe the effect of exciton–LO-phonon interaction by means of an effective potential between an electron and a hole as first derived by Pollmann and Büttner using an exciton–bulk-optical-phonon Hamiltonian. Our calculations lead to the values of the binding energies of excitons which agree very well with those obtained by Zheng and Matsuura who consider an exciton interacting with confined-LO phonons, interface phonons, and half-space phonons. Our method has the great advantage over that followed by Zheng and Matsuura of being simpler, more efficient to use and is much easier to generalize to include the effects of external perturbations such as electric and magnetic fields. We compare the results of our calculations with available experimental data in a few representative polar quantum well structures and find a very good agreement. We show that a proper accounting for the exciton-phonon interaction in highly ionic quantum well structures is essential for understanding the experimental data.

ACKNOWLEDGMENT

One of the authors (K.K.B.) would like to thank G. Coli for useful discussions.

*Electronic address: senger@physics.emory.edu

¹B. Urbaszek, A. Balocchi, C. Bradford, C. Morhain, C.B. O'Donnell, K.A. Prior, and B.C. Cavenett, *Appl. Phys. Lett.* **77**, 3755 (2000).

²R. Cingolani, L. Calcagnile, G. Coli, R. Rinaldi, M. Lomascolo, M. DiDio, A. Franciosi, L. Vanzetti, G.C. LaRocca, and D. Campi, *J. Opt. Soc. Am. B* **13**, 1268 (1996).

³*Numerical Data and Functional Relationships in Science and Technology*, edited by O. Madelung, Landolt-Börnstein, New Series, Group III, Vol. 17 (Springer-Verlag, New York, 1982).

⁴A. Ohtomo, M. Kawasaki, T. Koida, K. Masubuchi, H. Koinuma, Y. Sakurai, Y. Yoshida, T. Yasuda, and Y. Segawa, *Appl. Phys. Lett.* **72**, 2466 (1998).

⁵A. Ohtomo, M. Kawasaki, I. Ohkubo, H. Koinuma, T. Yasuda, and Y. Segawa, *Appl. Phys. Lett.* **75**, 980 (1999).

⁶T. Makino, C.H. Chia, N.T. Tuan, H.D. Sun, Y. Segawa, M. Kawasaki, A. Ohtomo, K. Tamura, and H. Koinuma, *Appl. Phys. Lett.* **77**, 975 (2000).

⁷T. Makino, C.H. Chia, N.T. Tuan, H.D. Sun, Y. Segawa, M. Kawasaki, A. Ohtomo, K. Tamura, and H. Koinuma, *Appl. Phys. Lett.* **77**, 1632 (2000).

⁸A. Ohtomo, K. Tamura, M. Kawasaki, T. Makino, Y. Segawa, Z.K. Tang, G.K.L. Wong, Y. Matsumoto, and H. Koinuma, *Appl. Phys. Lett.* **77**, 2204 (2000).

⁹T. Makino, N.T. Tuan, H.D. Sun, C.H. Chia, Y. Segawa, M. Kawasaki, A. Ohtomo, K. Tamura, T. Suemoto, H. Akiyama, M. Baba, S. Saito, T. Tomita, and H. Koinuma, *Appl. Phys. Lett.* **78**, 1979 (2001).

¹⁰H.D. Sun, T. Makino, N.T. Tuan, Y. Segawa, M. Kawasaki, A. Ohtomo, K. Tamura, and H. Koinuma, *Appl. Phys. Lett.* **78**, 2464 (2001).

¹¹G. Coli and K.K. Bajaj, *Appl. Phys. Lett.* **78**, 2861 (2001).

¹²H.D. Sun, T. Makino, Y. Segawa, M. Kawasaki, A. Ohtomo, K. Tamura, and H. Koinuma, *J. Appl. Phys.* **91**, 1993 (2002).

¹³H.D. Sun, Y. Segawa, M. Kawasaki, A. Ohtomo, K. Tamura, and H. Koinuma, *J. Appl. Phys.* **91**, 6457 (2002).

¹⁴T. Makino, K. Tamura, C.H. Chia, Y. Segawa, M. Kawasaki, A. Ohtomo, and H. Koinuma, *Appl. Phys. Lett.* **81**, 2355 (2002).

¹⁵C.H. Chia, T. Makino, K. Tamura, Y. Segawa, M. Kawasaki, A. Ohtomo, and H. Koinuma, *Appl. Phys. Lett.* **82**, 1848 (2003).

¹⁶T. Makino, K. Tamura, C.H. Chia, Y. Segawa, M. Kawasaki, A. Ohtomo, and H. Koinuma, *J. Appl. Phys.* **93**, 5929 (2003).

¹⁷V. Fiorentini, F. Bernardini, F. Della Sala, A. Di Carlo, and P. Lugli, *Phys. Rev. B* **60**, 8849 (1999).

¹⁸M. Leroux, N. Grandjean, J. Massies, B. Gil, P. Lefebvre, and P. Bigenwald, *Phys. Rev. B* **60**, 1496 (1999).

¹⁹A. De Nardis, V. Pellegrini, R. Colombelli, F. Beltram, L. Vanzetti, A. Franciosi, I.N. Krivorotov, and K.K. Bajaj, *Phys. Rev. B* **61**, 1700 (2000).

²⁰R. Cingolani, P. Prete, D. Greco, P.V. Giugno, M. Lomascolo, R. Rinaldi, L. Calcagnile, L. Vanzetti, L. Sorba, and A. Franciosi, *Phys. Rev. B* **51**, 5176 (1995).

²¹J. Pollmann and H. Büttner, *Solid State Commun.* **17**, 1171 (1975).

²²J. Pollmann and H. Büttner, *Phys. Rev. B* **16**, 4480 (1977).

²³M. Kumagai and T. Takagahara, *Phys. Rev. B* **40**, 12 359 (1989).

²⁴R. Zheng and M. Matsuura, *Phys. Rev. B* **58**, 10 769 (1998).

²⁵J.M. Luttinger, *Phys. Rev.* **102**, 1030 (1956).

²⁶A. Baldareschi and N.O. Lipari, *Phys. Rev. B* **3**, 439 (1971).

²⁷G. Behnke, H. Büttner, and J. Pollmann, *Solid State Commun.* **20**, 873 (1976).

²⁸R.T. Senger and A. Erçelebi, *J. Phys.: Condens. Matter* **9**, 5067 (1997).

- ²⁹R.L. Greene, K.K. Bajaj, and D.E. Phelps, Phys. Rev. B **29**, 1807 (1984).
- ³⁰H.W. Hölscher, A. Nöthe, and C. Uihlein, Phys. Rev. B **31**, 2379 (1985).
- ³¹H.X. Fu, L.W. Wang, and A. Zunger, Phys. Rev. B **57**, 9971 (1998).
- ³²J. Puls, V.V. Rossin, F. Henneberger, and R. Zimmermann, Phys. Rev. B **54**, 4974 (1996).
- ³³*Semiconductor—Basic Data*, edited by O. Madelung (Springer, Berlin, 1996).
- ³⁴N.T. Pelekanos, J. Ding, M. Hagerott, A.V. Nurmikko, H. Luo, N. Samarth, and J.K. Furdyna, Phys. Rev. B **45**, 6037 (1992).
- ³⁵S. Choopun, R.D. Vispute, W. Yang, R.P. Sharma, T. Venkatesan, and H. Shen, Appl. Phys. Lett. **80**, 1529 (2002).
- ³⁶L.C. Andreani and A. Pasquarello, Phys. Rev. B **42**, 8928 (1990).
- ³⁷N. Mori and T. Ando, Phys. Rev. B **40**, 6175 (1989).
- ³⁸H. Rucker, E. Molinari, and P. Lugli, Phys. Rev. B **44**, 3463 (1991).
- ³⁹L.F. Register, Phys. Rev. B **45**, 8756 (1992).
- ⁴⁰See for example, S.B. de-Leon and B. Laikhtman, Phys. Rev. B **67**, 235315 (2003).
- ⁴¹I. Vurgaftman, J.R. Meyer, and L.R. Ram-Mohan, J. Appl. Phys. **89**, 5815 (2001).